Nonlinear Effects for Sidelobe Characteristics of Pulse Radars

Takashi Shiba, Masato Watanabe, Masahiro Ishii, Manabu Akita and Takayuki Inaba
The University of Electro-Communications, Graduate school of Informatics and Engineering,
1-5-1 Chofugaoka, Chofu-shi, Tokyo, Japan

***Abstract*—Nonlinear effects on correlation sidelobes of receiver signals for pulse radars, which were UWB pulse radar, pulse compression radar and mainly phase coded high pulse repetition frequency (PCHPRF) radar were discussed. Sidelobes of pulse radars increases in the case of nonlinear system with some other radio frequency (RF) parameters. We investigated on the parameters verified decision parameters for these sidelobe characteristics by using RF simulation method considering nonlinear effects.**

***Index Terms*—nonlinear, pulse radar, correlation sidelobe, RF-circuit**

I. Introduction

Radar systems are generally used in military and consumer markets. The radar has attracted as car sensor in Intelligent Transport Systems (ITS) because of high weatherability recently. Information of target range and velocity is obtained by using radar in such type of systems. These parameters correspond to delay time and Doppler shift of frequency especially in pulse radar including Pulse Doppler radar. So it is easy to obtain this information by using these type radars. Range resolution is decided by pulse width for simple UWB pulse radar [1]. Pulse compression radar is developed for purpose of a high range resolution. Aperiodic correlation code and some guard interval are needed in some types of pulse compression radars [2] for avoiding misdetection due to the pulse repetition. Periodic correlation code without guard interval is used for PCHPRF radar, which has been proposed by our research group [3] [4]. In this radar, we employ FFT and short term correlation, which is realized by relatively low computational load, for PCHPRF demodulation. RF front-end circuits near antenna of these pulse radar systems generally have some nonlinear characteristics, which affect on the correlation sidelobe. Correlation sidelobe performances affected by nonlinear are discussed in this paper.

II. Experimental Results of PCHPRF and Pulse Compression Radars

A. Flexible Radar System

At First, we illustrated whole our measurement system in Fig.1. We were able to make several waveforms by using arbitrary waveform generator and to measure several kinds of pulse radar systems by using this system. We also prepared RF up and down convertor (intermediate frequency IF: 8 GHz, RF: 79.5 GHz) with some bandpass and low pass filters, some mixers and some amplifiers. The performance of these RF systems was adjusted for standard of 79 GHz band high-resolution radar. We measured 3 types of pulse radar, PCHPRF radar, pulse compression radar of correlation code type and UWB pulse radar.

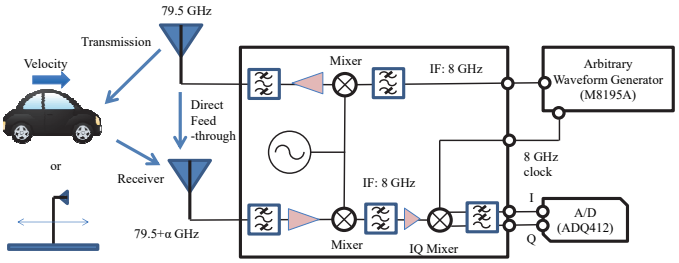

Fig. 1. 79 GHz milimeter wave flexible radar system.

B. PCHPRF Radar

We show the results of PCHPRF radar first. In the experiment on an anechoic chamber, we used Ipatov code [5] as a correlation code sequence, 624 chips as a correlation code length, 1 ns as pulse width, 1/4 as pulse duty and a static corner reflector as the target. The results are shown in Fig. 2. The results of Fig. 2 correspond to coherent pulse interval *CPI*=10 ms as usual condition and the number of code cycle *Nc*=4096. Horizontal axis corresponds to the products of signal delay time τ and sampling frequency *fs* and vertical axis corresponds to absolute value square of correlation signal *s* represented by a dBm unit. The highest peak corresponds to direct feedthrtough and second one corresponds to the target. This result is the range profile associated with zero Doppler frequency bin, because target is static in the experiment.

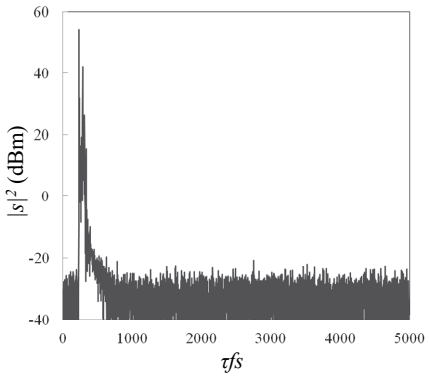

Fig. 2. Experimental Results of Correlation Signals for PCHPRF Radar (*Nc*=4096).

The local maximum value of sidelobe *Sl* is defined by equation (1) as described below.

$$Sl = \max(|s_j|)_{j \cdots j+Ns-1} \quad (1)$$

Here s_j and *Ns* are each signal complex value in sidelobe area and the number of signal in sidelobe area, respectively. Sidelobe area is chosen from no correlation main signal area, *j*=1000 to 4000 in this case. Thick line corresponds to the power mean value of sidelobe *Sm*. *Sm* is defined by equation (2) as described below.

$$Sm = \sqrt{\frac{\sum_{j}^{j+Ns-1} |s_j|^2}{Ns}} \quad (2)$$

Sl=-20.9 dBm (*Peak/Sl*=74.9 dB) and *Sm*=-31.7 dBm (*Peak/Sm*=85.8 dB) are obtained in this case. Increasing quantity of sidelobe level by nonlinearity of system can not be observed because degradation quantity of sidelobe level is low in this case. Therefore, we also measured in condition of *CPI*=40 ms (*Nc*=16384) to reduce noise level for nonlinear effect observation. The results are shown in Fig. 3. Several subpeaks in sidelobe area are observed in this second case. Skirt characteristics near peaks are generated by dispersive characteristics of systems. *Sl*=-23.8 dBm (*Peak/Sl*=77.8 dB) and *Sm*=-36.4 dBm (*Peak/Sm*=90.4 dB) are obtained in this second case.

Relationships between the number of cyclic code and each sidelobe levels for PCHPRF Radar are also plotted in Fig. 4.

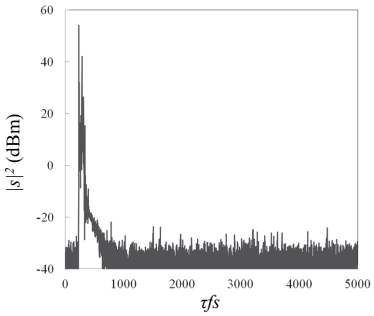

Fig. 3. Experimental Results of Correlation Signals for PCHPRF Radar (*Nc*=16384).

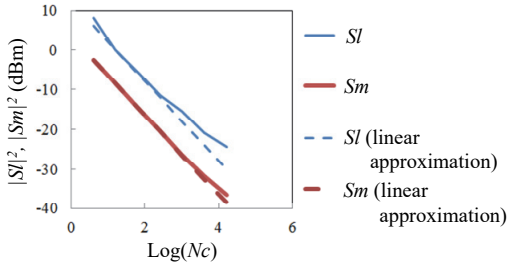

Fig. 4. Experimental Relation between The Number of Cyclic Code and Sidelobe Levels for PCHPRF Radar.

Thin lines are corresponding to local maximum value of sidelobe, *Sl* and thick lines are corresponding to power mean value of sidelobe *Sm*. Broken lines also correspond to linear approximation having a square root slope of *Nc* because the noise power is in inverse proportional to *Nc* if the sidelobe area consists of noise component only. In high *Nc* area, maximum value of sidelobe does not fit to the linear approximation. The disagreement were caused by spike subpeaks which were made by nonlinear and/or other causes except for noise. (See chapter IV.)

C. Pulse Compression Radar

We show the result of correlation code type pulse compression radar next. We used Complimentary Phase Code (CPC) as aperiodic correlation code, 512 chips as correlation code length. Other parameters and conditions are the same as the case of PCHPRF. The results are shown in Fig. 4. The results of Fig. 4 corresponds to *CPI*=10 ms (*Nc*=2496) as a usual case. Two peaks correspond to the same as Fig. 3. Skirt characteristics near peaks are also generated by dispersive characteristics of RF systems. Sidelobe area is chosen as *j*=500 to 2500 in this case, because *Nc* corresponding to *CPI* is lower than former case. *Sl*=-7.5 dBm (*Peak/Sl*=64.9 dB) and *Sm*=-25.3 dBm (*Peak/Sm*=82.8 dB) are obtained in this case. Some local swelling area of sidelobe in low delay time is observed in this case.

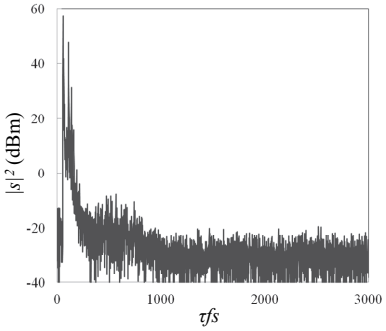

Fig. 5. Experimental Results of Correlation Signals for Pulse Compression Radar (*Nc*=2496).

D. UWB Pulse Radar

We also show the result of UWB Pulse radar. We set the same condition, 1/4 as pulse duty and static corner reflector as target as other radars. The results are shown in Fig. 5. The results of Fig. 5 corresponded to 10ms *CPI* (*Nc*=4096) as usual case. These results are also associated with zero Doppler bin.

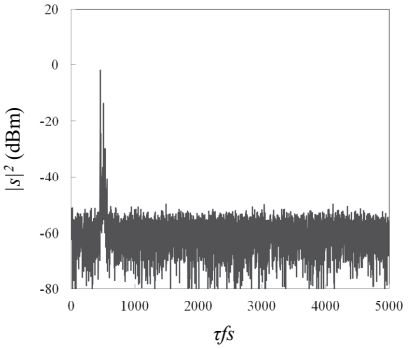

Fig. 6. Experimental Results of Received Signals for UWB Pulse Radar (*Nc*=16384).

Two peaks correspond to the same as the case of PCHPRF. Sidelobe area is chosen as j=1000 to 4000 as in the case with PCHPRF. *Sl*=-50.0 dBm (*Peak/Sl*=47.9 dB) and *Sm*=-58.7 dBm (Peak/Sm=56.7 dB) are obtained in this case. No increasing of sidelobe as subpeak or local increasing area was found because the sidelobe level was higher than the former two cases. That is caused by the lower S/*N* improvement by signal processing of the case than that of the former two cases.

III. Simulation Results

A. Simulation Method

We simulated received signals for Pulse Radars by using RF simulation methods [6]. Simulation was set according to practical RF circuit arrangement. Especially, we represented nonlinear effects using intercept point parameters for high power amplifier near transmitter antenna. 2nd order output intercept point *OIP2*=37.1 dBm, 3rd order output intercept point *OIP3*=26.2 dBm and noise figure *NF*(receiver total)=4.9 dB and receiver total gain *G*=50 dB of measured and specification values are used for simulation. And we used the below noise relation shown in eq. (3) to reduce simulation time for high *Nc* case.

$$No = \frac{Ni}{\sqrt{Nc}} \tag{3}$$

Here, *Ni* is the initial noise level, *Nc* is the number of cyclic correlation code, *No* is the result value of noise, respectively.

We simulated only for PCHPRF and pulse compression radar because sidelobe of UWB pulse radar was higher than others. Sidelobe degradation of UWB pulse radar by nonlinear can not be observed because of less process gain than others. RF simulations were original Fortran source code and baseband signal processing parts were original Mathcad code. Measurement data format from A/D convertor and simulation data format were adjusted each other, therefore the same baseband signal process were used for both experiments and simulations.

B. PCHPRF Radar

Simulation results corresponding to the case of *Nc*=16384 are shown in Fig. 7. *Sl*=-23.4 dBm *(Peak/Sl*=77.6 dB) and *Sm*=-37.3 dBm (*Peak/Sm*=91.4 dB) are obtained in this simulation case. Compared with Fig. 3 and Fig. 7, a good agreement between the experiment and the simulation is obtained, especially the difference between experiments and simulation of sidelobe (*Sl,Sm*) are lower than 1.0dB. These sharp subpeaks are also similar .

We also simulated the relation between sidelobe and *Nc*. The comparison between experiment and simulation is shown in Fig.8. Solid lines are the same as in Fig. 4. Dotted lines are simulation results. Dotted thin line is simulation for maximum value, dotted thick lines are simulations for power mean values, respectively. A good agreement between experiments and simulations was obtained as shown in Fig. 8. The difference between experiments and simulation of sidelobe (*Sl,Sm*) are lower than 3.0 dB in measured and simulation area. It is thought that these simulation methods were verified by these good agreements.

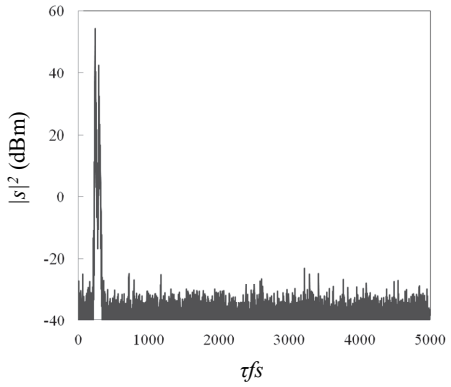

Fig. 7. Simulation Results of Correlation Signals for PCHPRF Radar (*Nc*=16384).

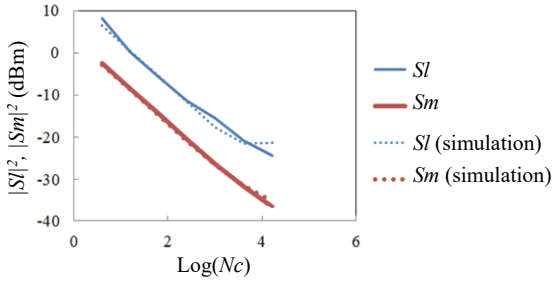

Fig. 8. Experimental and Simulation Results about Relation of The Number of Cyclic Code and Sidelobe Levels for PCHPRF Radar.

C. Pulse Compression Radar

Simulation results for pulse compression radar are shown in Fig. 9. *Sl*=-6.5 dBm (*Peak/Sl*=65.0 dB) and *Sm*=-22.3 dBm (*Peak/Sm*=80.8 dB) are obtained in this simulation case. The difference between experiments and simulation of sidelobe (*Sl,Sm*) are lower than 3.0 dB. The results of experiments and simulation are similar, especially swelling area. The result shown in Fig. 9 is almost same as Fig. 5. It also thought that these simulation methods can be used for the analysis of sidelobe in this type of radar.

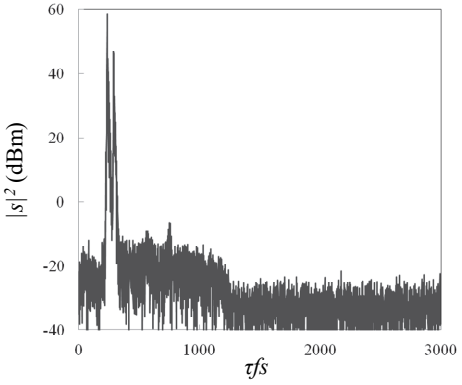

Fig. 9. Simulation Results of Correlation Signals for Pulse Compression Radar (*Nc*=2496).

IV. Discussion of Decision Parameters Related for Sidelobes

Using this RF simulator, several parameters were tested for sidelobe level. We found continuous wave (CW) leak, dispersive frequency characteristics of circuit and nonlinear effects except for noise level were strongly related to these sidelobes in both PCHPRF and Pulse compression radar case. Especially 3rd order intercept point was effective for PCHPRF radar and 2rd order intercept point was effective for pulse compression radar. Confirmation method for dispersive frequency characteristics is shown in Fig. 10 for example. The left flow indicates normal simulation as shown in Fig. 7 and the right flow also indicates this confirmation flow (simulation A). If sidelobe characteristics is not related with dispersive frequency characteristics of the system and nonlinear effect, normal simulation and simulation A become the same results. The results of simulation A is shown in Fig. 11. All subpeaks in sidelobe disappear in results by simulation A. Therefore, dispersive characteristics before nonlinear amplifier are effective to sidelobe characteristics. Other parameters (CW leak level before nonlinear portion and 2nd and 3rd intercept point) were also confirmed by similar calculation.

All origins/factors of increasing sidelobes were mainly feedthrough signals. All experimental results and simulations in this paper were only for a static corner reflector as a target. We confirmed that these subpeaks disappear for mobile target. However, these subpeaks in sidelobe by nonlinearity of system will appear in the case where there is a target located in the close range from radar with strong reflection signal having the same velocity. Consequently the below countermeasures for degradation of sidelobe were considered.

(1) High linearity power amplifier

(2) Suppression of dispersivity before power amplifier.

(3) Suppression of CW leak before power amplifier.

(4) High isolation characteristics between transmitter and receiver antenna ports. (Only for static target.)

V. Conclusion

Nonlinear effects on sidelobe characteristics were discussed. Nonlinearity of frontend, CW leak before nonlinear effect and dispersivity of circuit before nonlinear effect were strongly related for PCHPRF radar and pulse compression radar. These results were verified by RF simulation.

Acknowledgment

This research was supported by Research and Development for Expansion of Radio Wave Resources of Ministry of Internal Affairs and Communications (MIC).

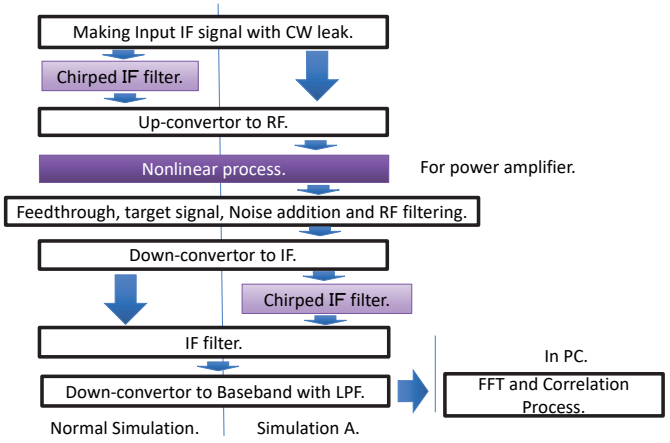

Fig. 10. Difference of Simulation Flow for dispersive effect of PCHPRF Radar.

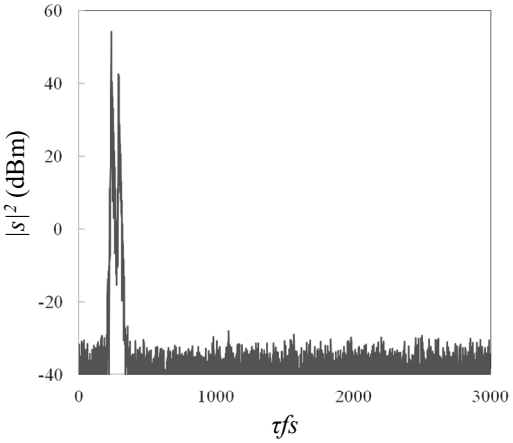

Fig. 11. Results of Correlation Signals by Simulation A for PCHPRF Radar (Nc=16384).

References

[1] V. Jain, S. Sundararaman and P. Heydari., "A 22-29-GHz UWB Pulse-Radar Receiver Front-End in 0.18-µm CMOS", IEEE Trans. on Microwave Theory and Tech., vol.57, No. 8, pp.1904-2009, Aug. 2009.

[2] Stimson, G.W., "Introduction to Airborne Radar, 2nd Edition", Scitech. Publishing Mendham, 1998.

[3] Levanon, N., "Mitigating Range Ambiguity in High PRF Radar using Inter-Pulse Binary Coding," Aerospaceand Electronic Systems, IEEE Transactions on , vol.45, no.2, pp.687-697, April 2009.

[4] M. Watanabe, M. Akita and T. Inaba, "Enhancement of Range Detection by using Inter-pulse Cyclic Phase Coding in UWB impulse Radar," The IEICE Transactions on Communications vol. J97-B No.7, pp.687-697, July 2014.

[5] V. P. Ipatov, "Ternary sequences with ideal autocorrelation properties", Radio Eng. Electron. Phys., vol. 24, pp.75-79, 1979.

[6] T. Shiba, M. Watanabe, M. Ishii, M. Akita T. Inaba, "Development of RF Simulation for PC-HPRF Radar", IEICE Technical Report MW2015-134, pp.7-12, 2016 (in Japanese).